Biophysical Chemistry 165–166 (2012) 79–86

Contents lists available at SciVerse ScienceDirect

Biophysical Chemistry

journal homepage: http://www.elsevier.com/locate/biophyschem

Structure and dynamics of β-lactoglobulin in complex with dodecyl sulfate and laurate: A molecular dynamics study

Martiniano Bello [a,*], Gabriel Gutiérrez [b], Enrique García-Hernández [b,**]

[a] Departamento de Medicina Molecular y Bioprocesos, Instituto de Biotecnología, Universidad Nacional Autónoma de México, Cuernavaca, Morelos 62210, Mexico
[b] Instituto de Química, Universidad Nacional Autónoma de México, Circuito Exterior, Ciudad Universitaria, 04360 México, D. F., Mexico

HIGHLIGHTS

- βlg interacts distinctly with cognate ligands dodecyl sulfate (DS) and laurate (LA).
- Both polar and apolar interactions seem to be better optimized in the complex βlg-DS.
- The interaction differences yield distinct effects on the structural dynamics of βlg.
- Results help to rationalize the "nonclassical" hydrophobic binding of βlg to DS.
- And the switch to a "classical" hydrophobic signature for βlgLA complex.

GRAPHICAL ABSTRACT

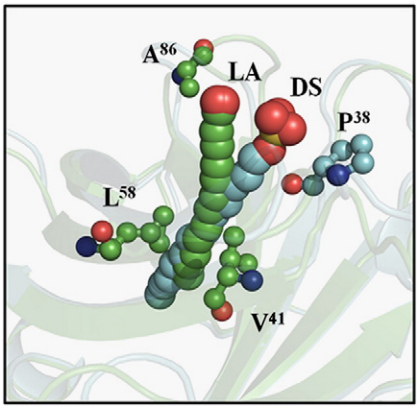

ARTICLE INFO

Article history:
Received 21 February 2012
Received in revised form 16 March 2012
Accepted 17 March 2012
Available online 24 March 2012

Keywords:
Protein-lipid complex
Classical hydrophobic effect
Nonclassical hydrophobic effect
Molecular dynamics simulations
Principal component motions

ABSTRACT

Bovine β-lactoglobulin (βlg) is able to recognize a wide variety of hydrophobic ligands. Although binding promiscuity is characteristic of highly hydrophobic interactions, the structural plasticity of the βlg binding cavity entrance seems to be crucial for the interaction with polar moieties of different ligands. On the other hand, thermodynamic studies have shown that βlg can associate to cognate ligands with distinctly different binding energetics, as in the case of the closely related molecules lauric acid (LA) and dodecyl sulfate (DS). In the recognition of LA, βlg shows a classical hydrophobic signature (entropically driven), whereas the interaction of βlg with DS exhibits a nonclassical hydrophobic signature (enthalpically driven). To gain insights into these opposed binding behaviors, MD simulations were carried out on βlg in apo-form and bound to DS or LA. Overall, the results suggested that the distinct energetic signatures of these ligands come from distinct optimizations of both hydrophilic and hydrophobic contacts with the protein.

1. Introduction

Bovine β-lactoglobulin (βlg) is one of the most thoroughly studied members of the lipocalin family, a large group of proteins involved, among other functions, in the transport of small hydrophobic molecules [1]. In spite of this, many of its properties remain to be unveiled, including its biological function. The 3D-structure of this lipocalin has been solved by X-ray crystallography and/or NMR spectroscopy in a variety of conditions, including different pH values [2–4], ionic strengths [5] and in complex with different ligands [6,7]. It is constituted of nine antiparallel β-strands (βA to βI) and a three-turn α-helix. Eight β-strands (βA to βH) give shape to a stable antiparallel β-barrel, with a conical central cavity, or calyx, that functions as the primary ligand-binding site. The entrance of the cavity is flanked by the very flexible loops AB, CD, EF and GH, whereas the

* Corresponding author. Tel.: +52 777 311 4900.
** Corresponding author. Tel.: +52 55 56 22 44 24; fax: +52 55 56 16 22 03.
E-mail addresses: bmartini@ibt.unam.mx (M. Bello), egarciah@unam.mx (E. García-Hernández).

0301-4622/$ – see front matter © 2012 Elsevier B.V. All rights reserved.
doi:10.1016/j.bpc.2012.03.009

more rigid loops BC, DE and FG are located at the bottom of the β-barrel.

Several structures of ligand-bound forms of βlg have been reported. Qin et al. [6] solved the structure of βlg with Br-dodecanoic acid. Shortly after, Wu et al. [7] reported the structure of the βlg-palmitic acid complex (βlgPA). In both structures, the ligand aliphatic tail is immersed in the hydrophobic cavity, while the carboxylate group, highly exposed to the solvent, interacts with polar residues at the cavity entrance. More recently, the structures of βlg in complex with retinol [8], retinoic acid [8], vitamin D3 [9], caprylic acid [10], and capric acid [10] were reported.

βlg adopts a number of conformations as a function of pH. Below pH 3, the lipocalin is mainly monomeric, whereas at neutral pH it forms weak non-obligate homodimers [11,12]. At pH values between 6 and 8, it undergoes a number of conformational changes, known collectively as the "Tanford transition" [2,4]. This transition, triggered by the change in the ionization state of the anomalously high-pKa Glu^{89}, modifies the conformation of the loop EF. Under acidic conditions, the loop closes the cavity entrance, while at higher pH, it folds back to leave the interior exposed. Thus, the loop seems to serve as a lid for controlling the access of ligands to the calyx. In fact, in all the βlg-ligand complex structures solved so far, the loop EF is in the open conformation.

Insightful studies on the dynamics behavior of βlg have appeared in the literature. Fogolari et al. [13] and Uhrínová et al. [3] solved the NMR structure of monomeric βlg at acid pH (<3). Determinations of solution structures at higher pH values were precluded due to the observation of too broad signals, a situation that later was shown to be due to the rapid monomer–dimer equilibrium that takes place at pH > 3.5. The signal-broadening problem was elegantly solved by Sakurai and Goto [14], who engineered a single mutant βlg (A34C), which forms a disulfide bond at the dimer interface. Although the covalent link induced some local perturbations, the overall subunit conformation seems to be unaffected. Comparison of the NMR structures showed that acid-induced dissociation elicits no large changes in the overall structure of the subunits, although the dynamics of some local regions of the polypeptide chain are significantly modified. Titration experiments monitored by NMR spectroscopy revealed that while the dynamics of residues at the bottom of the binding cavity is marginally affected by the presence of the ligand, several residues lying at the cavity entrance region, particularly in the loops EF and GH and the β-strand D, increase their mobility [15,16]. This plasticity at the calyx mouth has been argued to be the basis for the promiscuous binding ability of the lipocalin [15].

Several genetic variants of βlg have been identified in cow's milk, variants A and B being the most prevalent. These variants differ at only two positions in the polypeptide chain: 64 ($Asp_A \rightarrow Gly_B$) and 118 ($Val_A \rightarrow Ala_B$). The former position, located near the flexible CD loop, is highly exposed to the solvent. The latter position, at the β-strand H, is immersed in the hydrophobic cavity of the protein. Although the crystal structures of the variants show that these mutations do not cause any significant conformational difference, distinct properties have been documented, including stability, dynamic behavior, dimerization and ligand binding energetics, [17–19].

βlg is able to recognize a broad variety of hydrophobic compounds, with apparent binding constants ranging from 10^2 to 10^8 M^{-1} [17]. Detailed determinations of binding energetics have been a difficult task, due to the impractically low water solubility of most βlg ligands. This situation has precluded going deeper in the elucidation of the energetic basis of ligand recognition by βlg. In a recent calorimetric study, lauric acid (LA) and dodecyl sulfate (DS) were shown to be soluble enough to obtain reliable binding data [18]. Yet, it was necessary to use low protein concentrations in the calorimetric measurements, conditions under which βlg was mostly monomeric. Although the two ligands share similar chemical architectures, they showed largely distinct binding properties. ΔH_b and $T\Delta S_b$ for βlg (variant B) binding to LA were 1.6 and 9.4 kcal/mol (35 °C), respectively, while the corresponding parameters for binding to DS were −4.2 and 3.8 kcal/mol (30 °C), respectively. Therefore, LA binding exhibits the classical hydrophobic signature, while DS binding represents a case of nonclassical hydrophobic signature [20]. It is interesting to note that in spite of these distinctly different behaviors, enthalpic–entropic compensatory effects cause βlg to recognize both ligands with similar affinities ($K_b \sim 4–6 \times 10^5$ M^{-1}). This situation clearly illustrates the importance of decomposing the Gibbs free energy of binding into its enthalpic and entropic constituents, in order to unveil fundamental properties that could otherwise remain unnoticed.

To gain insights into the structural basis of βlg's different binding energetics to LA and DS, herein we present a MD simulation study of monomeric βlg in apo-form (βlg_{apo}) and complexed with lauric acid (βlgLA) or DS (βlgDS). The free monomer of βlg was used, since, as stated above, calorimetric binding parameters were obtained under conditions where that state was the most populated. It is to be recalled that at neutral pH, it has only been possible to solve the structure of βlg in dimeric form by either X-ray or NMR approaches. So, at the moment only MD techniques can be used to study the monomer with atomic resolution at neutral pH. Nevertheless, monomeric and dimeric subunits coexist nearly equimolar in cow's milk, suggesting that both states are physiologically relevant [18,21]. Overall, the results presented herein indicate that βlg interacts distinctly with the two ligands. The protein forms more cooperative and lasting hydrogen bonds with the sulfate group than with the carboxylate group. Besides, the DS hydrophobic tail penetrates deeper into the binding cavity, allowing this ligand to establish a larger number of hydrophobic contacts than LA. Hence, the more favorable DS binding enthalpy seems to arise from better optimization of both polar and apolar interactions. On the other hand, the lesser penetration of the aliphatic tail as well as the establishment of fewer contacts by the polar moiety are consistent with the higher entropy binding of LA.

2. Methods

βlg variant B was used in all simulations. The structure of βlg_{apo} has been solved several times. We chose the one reported by Oliveira et al. [19] which, solved at pH 7.9, shows the loop EF in the open conformation (pdb entry 1B8E). The LA-complex structure was built from the βlgPA X-ray coordinates (pdb entry 1B0O) [7], by removing the fatty-acid atoms C13 to C18. The βlgDS structure has not yet been solved experimentally. Nevertheless, there is convincing evidence that DS positions itself similarly to LA inside the binding cavity [18,22,23]. Accordingly, the structure of βlgDS was built from βlgLA, by replacing the carboxylate atoms O1 and O2 with the sulfate atoms S, O1, O2, O3 and O4, while preserving unaltered the aliphatic tail.

MD simulations were performed using the GROMACS 4.0.5 software, with the GROMOS 5346 force field [24]. Protonation state was the same for all the structures: LYSH, ASP, GLU, HISA (ND1 protonation) or HISB (NE2 protonation) were used according to the optimal H-bonding conformation. The molecular topologies for LA and DS were obtained from the Dundee PRODRG Server [25]. A corresponding number of 7 sodium ions were placed in energetically favorable positions to neutralize the net charge of the system. MD simulation trajectories were calculated in a periodic dodecaedric box that extended 1 nm between the complex and the edge of the box. A simple point charge (SPC) water model was used [26].

Prior to MD simulations, internal constraints were relaxed by energy minimization, followed by 0.1 ns equilibration under position restraints of the carbon backbone atoms through a harmonic force constant of 1000 kJ mol^{-1} nm^{-1}. During the MD simulation runs, the LINCS algorithm was used to constrain the length of covalent bonds [27]. The SETTLE algorithm was used to constrain the water molecules [28]. The simulations were run under constant pressure and temperature, using the Berendsen's coupling algorithm [29]. A time step of 2 fs was used. Van der Waals forces were treated using a cutoff of 1.2 nm, while the long-range electrostatic forces (r > 1.2 nm)

were treated using the particle mesh Ewald method [30]. For all MD simulations, the first 10 ns were taken as equilibrium time and the last 40 ns were used for the analysis.

Root-mean-square deviations (RMSD) and root-mean-square fluctuations per residue (RMSF) were calculated taking the energy minimized structure as a reference. The principal components of the protein motion were determined from the diagonalization of the variance–covariance matrix [31], providing the amplitude and the direction of each concerted motion (i.e., the eigenvalues and the corresponding eigenvectors). The trajectories were projected on the eigenvectors with the largest eigenvalues, and images were generated of the two extreme protein backbone conformations for each of these motions. Average structures were calculated from the variance–covariance matrix of all protein atoms during the last 40 ns of the run, using the GROMACS program g_covar, and then they were regularized by energy minimization. A screening of the protein secondary structure was also performed for all the simulations, by using the definitions of the Dictionary of Protein Secondary Structure (DPSS). RMSD, RMSF, and the analysis of essential protein motions were calculated by means of programs contained in the GROMACS package. A least-squared fit was applied to eliminate roto-translation displacements with respect to the starting structure.

The number of intra and intermolecular hydrogen bonds were calculated for all the trajectories using a donor-acceptor atom cutoff distance of 0.35 nm and a donor-hydrogen-acceptor angle of less than 30°. Lifetimes of the hydrogen bonds between the polar moieties of LA or DS and the residues at the cavity entry were estimated by performing a time integration of the autocorrelation functions of bond occupation number. The radius of gyration (R_G) and apolar and polar solvent accessible surface areas (SASA) were determined throughout all the trajectories. The values obtained were averaged over the last 40 ns. Tools from the GROMACS package were used to determine H-bonds, R_G and SASA.

All the graphical representations were generated by PYMOL version 0.99rc6 [32].

3. Results and discussion

The structures of βlg_{apo}, βlgLA and βlgDS were submitted to 50-ns long MD simulations in explicit solvent. Several geometrical properties along the trajectory were determined to check equilibration of the systems. As shown in Fig. 1, the three structures reached an RMSD plateau within the first 5 ns of simulation. Therefore, all subsequent analyses were done excluding the initial 10-ns period, unless otherwise stated. The ligand-bound structures showed average RMSD (0.17 and 0.20 nm for βlgDS and βlgLA, respectively) somewhat smaller than that of the apo form (0.22 nm). Table 1 shows the average values of SASA, R_G, and the number of intra-protein hydrogen bonds (HB_{intra}). As judged from the corresponding standard deviations, these properties also indicate that the structures were stable during simulation. The three βlg forms shared almost identical values for SASA, R_G, and HB_{intra}. Furthermore, they showed similar contents of secondary structure (data not shown). Overall, these results indicate that a structural convergence plateau was reached during the simulation time, with no large conformational changes in the lipocalin upon ligand binding, a picture that is in agreement with previous experimental data [6,7].

3.1. Structural analysis of the binding site

3.1.1. Protein-ligand polar interactions

The X-ray structure of βlg in complex with palmitic acid (βlgPA) shows Lys^{60} and Lys^{69} forming a cooperative hydrogen bonding network with the carboxylate group of the fatty acid [7]. Furthermore, it has been reported that the absence of either of the two lysine residues may abolish the capacity of fatty acid binding. For instance, horse and donkey βlg have a Glu residue at position 60, while pig βlg has the same residue but at position 69. The three proteins are not able to bind fatty acids [33,34]. Thus, Lys^{60} and Lys^{69}, positioned at the calyx entrance, seem to play a significant role in stabilizing the interaction of βlg with fatty acids. Recent X-ray structures of bovine βlg bound to caprylic or capric acids show the ligands not interacting with any of the two lysines. Nevertheless, the interaction of any of these fatty acids with βlg seems to be very weak. The binding equilibrium constants for caprylic and capric acids are 11,000 and 6000 M^{-1}, respectively, while for LA it is 370,000 M^{-1} [10,18].

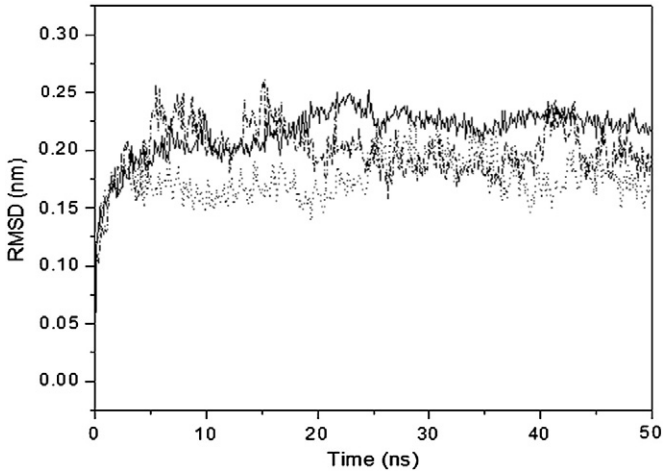

Fig. 1. Root mean square deviations (RMSD) of C^{α} atoms as a function of time. βlg_{apo} (black), βlgLA (dashed line) and βlgDS (dotted line).

Fig. 2 shows snapshots taken along the MD simulations, illustrating representative interactions that βlg establishes with the polar moiety of either DS (panels A–C) or LA (panels D–F). During the early equilibration state (<1 ns), the sulfate group interacted only with Lys^{60} (Fig. 2A). After that, it started to interact also with Asn^{88} and/or Asn^{90}, forming bi- and tridentate contacts (Fig. 2B–C). It is noteworthy that Asn^{88} and Asn^{90}, forming part of the loop EF, are located at the opposite side of the calyx entrance, in relation to Lys^{60} and Lys^{69}, which form part of βC and βD, respectively. In the case of LA, the carboxylate was initially interacting with both Lys^{60} and Lys^{69} (Fig. 2D). Nevertheless, between 0.8 and 15 ns of the overall simulation, it preferred to interact with only one lysine residue at a time (Fig. 2E). After that time, the carboxylate barely interacted with Lys^{69}, while establishing a new contact with Asn^{88} (Fig. 2F).

Fig. 3 shows the occurrence frequency of polar-to-polar intermolecular interactions, as extracted from the MD trajectories. For a considerable fraction of time, the ligand and protein were not hydrogen bonded to each other in the βlg complexes, although this situation lasted significantly longer in the LA complex. In contrast, the DS polar moiety established more frequent and cooperative hydrogen bonds with the protein. The sulfate group interacted simultaneously with two or three residues (Lys^{60}-Asn^{88}, Lys^{60}-Asn^{90}, Asn^{88}-Asn^{90} or Lys^{60}-Asn^{88}-Asn^{90}) around 40% of the time, while it made contact with only one of these residues for around one-third of the simulation. In contrast, the carboxylate's most recurrent interaction (~40% of the simulation) was with only one residue at a time (Lys^{60}, Lys^{69} or Asn^{88}), while it interacted simultaneously with two residues (Lys^{60}-Lys^{69} or Lys^{60}-Asn^{88}) for ~20% of

Table 1
Average geometrical properties of βlg forms along the MD simulations.

System	HB_{intra}	R_G (nm)	Apolar SASA (nm^2)	Polar SASA (nm^2)
βlg_{apo}	116 ± 5	1.50 ± 0.01	76 ± 2	55 ± 2
βlgLA	117 ± 3	1.50 ± 0.01	77 ± 1	54 ± 1
βlgDS	118 ± 3	1.50 ± 0.01	77 ± 1	55 ± 1

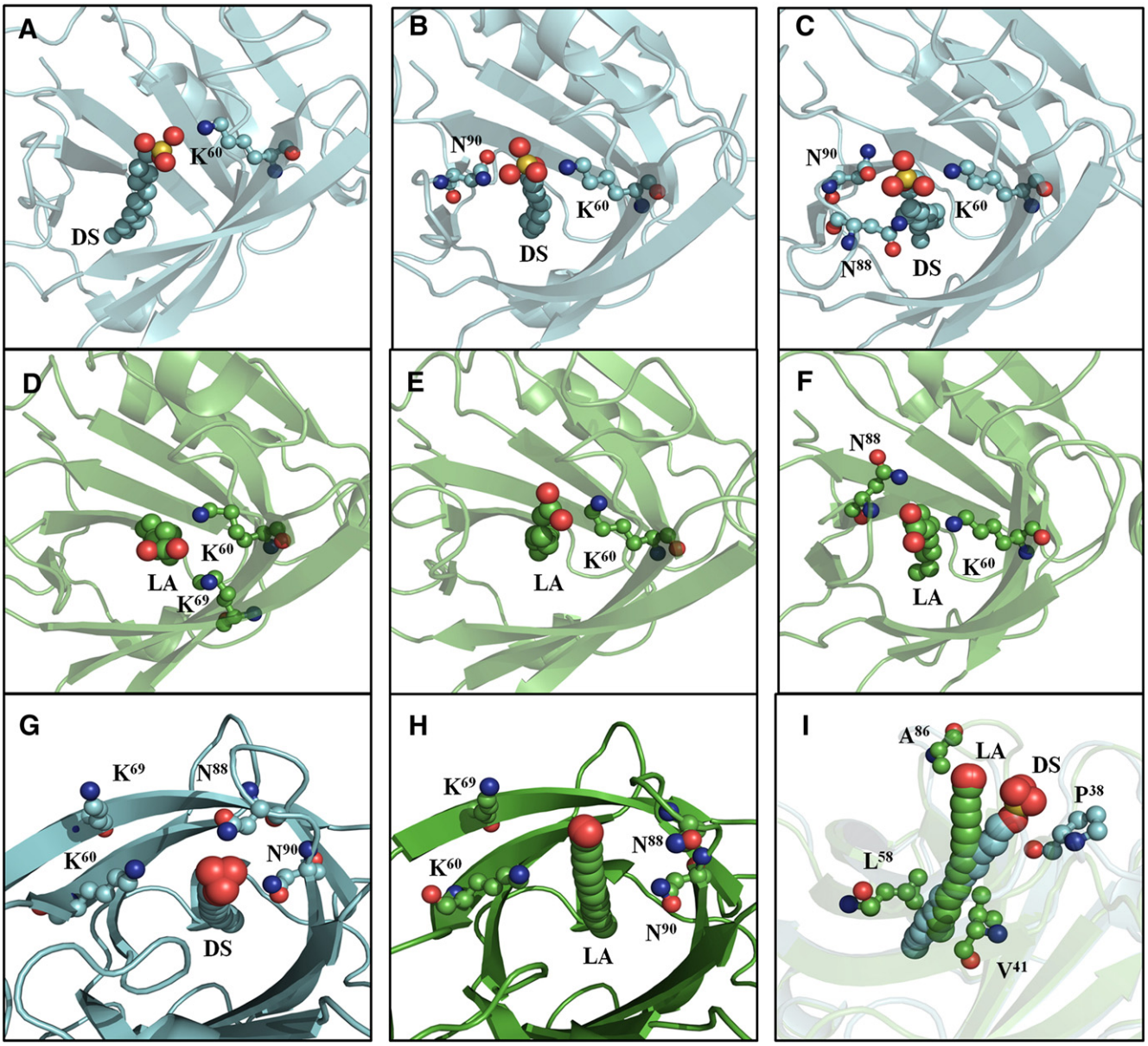

Fig. 2. Examples of βlg-ligand interaction modes. Time development of predominant contacts between polar residues at the βlg cavity entrance and the polar moiety of (A–C) DS and (D–F) LA. Average conformations of (G) DS and (H) LA inside the βlg binding cavity during the last 40 ns of MD simulation. (I) Comparison of the average conformations of DS and LA shown in panels (G) and (H).

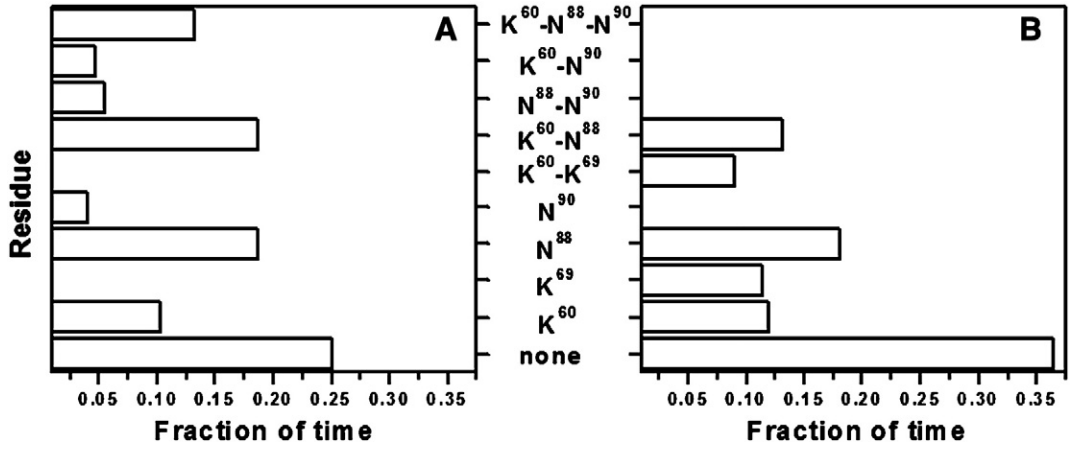

Fig. 3. Hydrogen-bonding frequency (fraction of time) of βlg residues with (A) DS or (B) LA. A hydrogen donor-acceptor pair distance of 0.35 nm was used to define a suitable hydrogen bonding contact.

the time. Tridentate interactions by this group were practically undetected throughout the simulation. Moreover, hydrogen-bond lifetimes were longer for DS (Lys^{60}, 1.2 ns; Asn^{88}, 1.7 ns; Asn^{90}, 1.8 ns) than for LA (Lys^{60}, 0.7 ns; Lys^{69}, 1.1 ns; Asn^{88}, 1.2 ns).

The results presented above indicate that the polar groups of LA and DS interact not only with Lys^{60} and/or Lys^{69}, as seen in the static X-ray structures of fatty acid-bound βlg, but are also able to make good contacts with polar residues located at the opposite side of the cavity entrance. Due to the different geometries of the polar groups, DS and LA interact distinctly with βlg residues. The MD data revealed that the bulkier sulfate group forms more cooperative and lasting polar-to-polar contacts with the protein, as opposed to those formed by the carboxylate group. Thus, although a carboxylate group has significant ability to form strong hydrogen bonds, and the sulfate anion is a weaker hydrogen-bond acceptor [35], the latter interacted better with the protein due to its capacity to accept a larger number of hydrogen atoms.

Figs. 2G–I compare the average positions along the simulations that DS and LA occupied inside the βlg calyx. It is clear that the polar groups prefer to lean on different parts of the calyx entrance. The orientation of the sulfate allowed it to form closer contacts with the residues of loop EF (Fig. 2G). In contrast, the carboxylate group kept closer to residues of βC and βD (Fig. 2H). Additionally, the aliphatic tails adopted distinct average orientations inside the binding cavity (Fig. 2I), namely, the DS aliphatic tail was more deeply immersed in the hydrophobic binding site.

3.1.2. Protein-ligand hydrophobic interactions

Analysis of the MD trajectories showed that in both βlgLA and βlgDS there was an extensive interaction of the ligand aliphatic tail with the host protein. Fig. 4 shows the hydrophobic contacts (cutoff distance 0.5 nm) for the corresponding average complex structures. DS was observed displacing deeper into the binding cavity relative to its initial position, within the first ns of equilibration time. In this new position, it was able to form more contacts than LA. 42 protein-ligand apolar contacts were formed in βlgDS, involving 15 protein residues in the interaction. In contrast, only 31 hydrophobic contacts were formed in βlgLA, involving 10 residues. This difference arose in part because the C1 and C2 atoms in βlgLA, being less buried, established fewer contacts with the protein. In contrast, these same atoms in βlgDS interacted closely with the side-chain carbon atoms of Pro^{38}, Leu^{39} and Asn^{90}. Additionally, C11 and C12 atoms in βlgDS contacted residues located deeper at the bottom of the binding pocket. In both complexes, Val^{92} was the residue that interacted with the largest number of ligand carbons. Due to the different extent of ligand penetration, Val^{92} interacted with DS's atoms C7-C11, and with LA's atoms C8-C12.

The X-ray structures of βlg bound to capryilic (C8) and capric (C10) acids were solved recently [10]. The structures revealed that the two fatty acids occupy different positions inside the βlg cavity. Capric acid is buried deeper in the binding cavity. Due to its closer proximity to the bottom of the calyx, it forms more hydrophobic contacts with the protein. However, its carboxylate group ends up being located too far away from the calyx entrance, hindering its interaction with any polar residue. In contrast, caprylic acid adopts a shallower position, allowing it to interact with Glu^{62} via a water molecule bridge, although establishing fewer hydrophobic contacts. Thus, as concluded by Loch et al. [10], a competition seems to take place between hydrophobic and polar interactions to determine the position of these fatty acids of short aliphatic chain. Fig. 5 shows the overlapped structures of βlg bound to DS and to caprylic and capric acids. It is interesting to note that DS seems to satisfy simultaneously both hydrophobic and polar interactions. Its aliphatic chain penetrates as deeply into the binding cavity as that of capric acid. At the

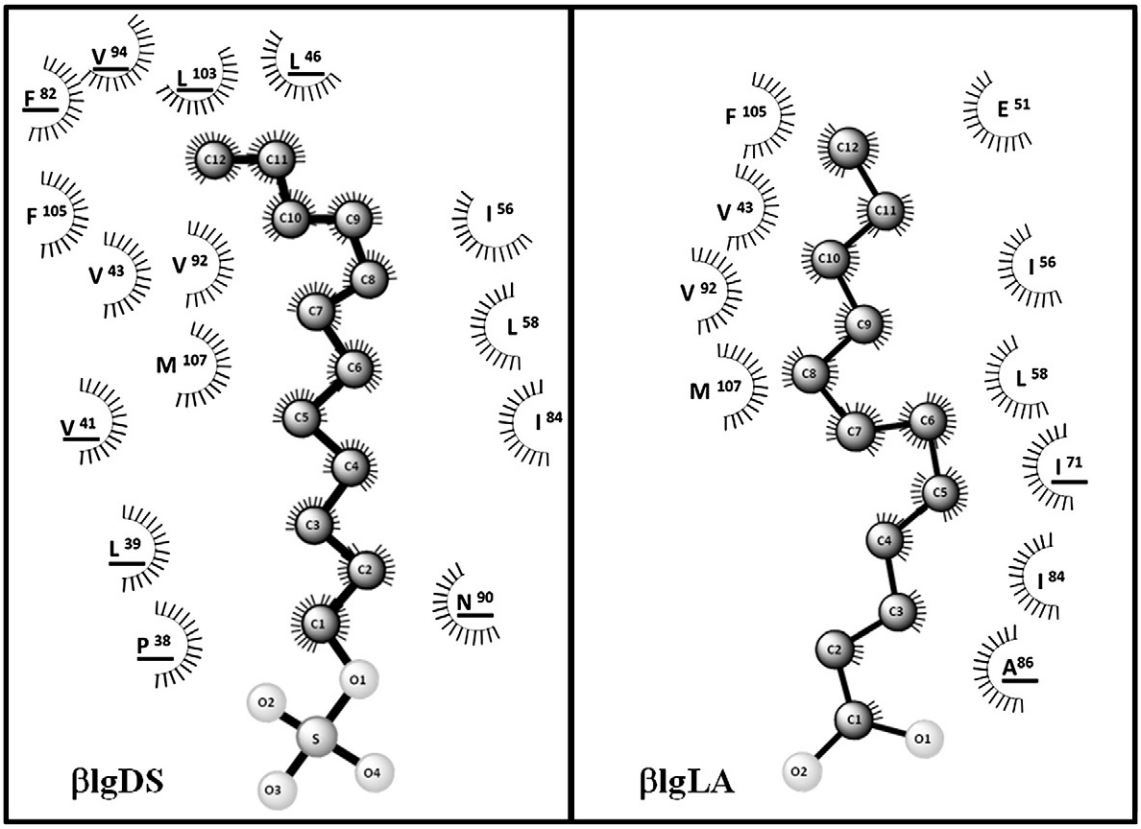

Fig. 4. Schematic representations of hydrophobic contacts of βlg with DS (left) or LA (right). The average conformations for the last 40 ns of simulations were used, taking an apolar-to-apolar atom pair distance cutoff of 0.5 nm. Protein residues involved in hydrophobic contact(s). Corresponding ligand atoms involved in hydrophobic contact(s). Residues forming hydrophobic contacts in only one of the two complexes are underscored. Drawings were generated using LIGPLOT v.4.5.3 [44] and ChemBioDraw V12.

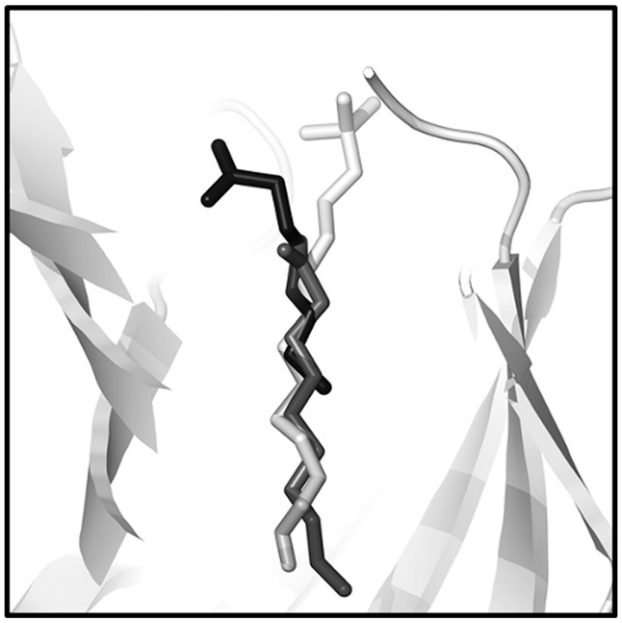

Fig. 5. Overlapping of DS (white), capric acid (gray) and caprylic acid (black) molecules inside the βlg binding cavity. The conformation of DS corresponds to the average conformation seen during the MD simulation. The conformations for caprylic and capric acids are those observed in the corresponding X-ray structures (pdb codes 3NQ3 and 3NQ9, respectively).

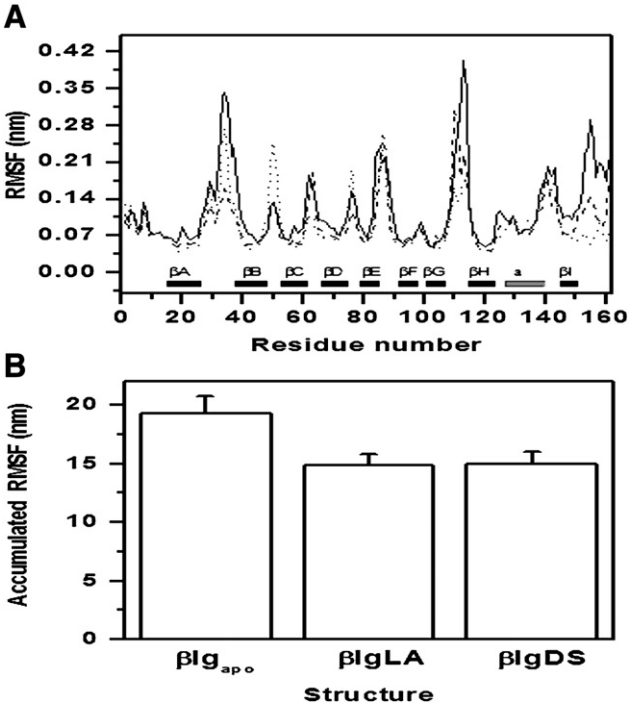

Fig. 6. (A) RMSF of βlg_{apo} (solid line), βlgLA (dotted line) and βlgDS (dashed line). (B) Accumulated RMSF values for the three βlg systems, obtained by summing up the RMSF values for all protein residues in panel A. The analysis was performed considering the α-carbon atoms for the last 40 ns of simulation.

same time, its bulkier polar group remains protruded enough to interact with polar residues at the calyx mouth.

No long-lived water molecules were observed inside the binding cavity in the three βlg structures throughout the simulation. Only Val[41], Ile[84] and Met[107], close to the cavity entrance, made contact with water molecules in βlg_{apo}. Nevertheless, the water molecules exhibited very low residence times (0.1–0.2 ns). These results agree with crystallographic and magnetic relaxation dispersion ^{13}C NMR data, revealing the absence of water molecules at the interior of the hydrophobic binding cavity in βlg_{apo} [2,36]. Furthermore, free energy calculations indicate that even when the calyx has enough room to accommodate several water molecules, the hydrophobic environment makes their incorporation energetically unfavorable [37]. Therefore, the burying of apolar carbons into the previously dehydrated binding cavity would be favored enthalpically, since the ligand does not have to displace water molecules from the protein surface upon binding. This situation has also been proposed for the major urinary protein, another lipocalin [38].

3.2. Conformational flexibility

MD results obtained in the present study show a complex dynamical behavior of βlg both in apo and ligand-bound forms. The RMSF analysis indicated that in general, the β-strands were the most rigid parts of the molecule (Fig. 6A). In the absence of the ligand, loops AB, CD, EF and GH, the helix α and the C-terminal region exhibited the highest mobility. According to NMR measurements, the loops CD, EF and GH undergo large fluctuations in the βlg dimer with unprotonated Glu[89], i.e., with the loop EF in open conformation [2]. At variance with our MD results, in those measurements more restricted movements were observed for the loop AB, which forms part of the dimer interface. This discrepancy is most probably due to the fact that the monomer was used in the present study. Large fluctuations of the loop AB and the C-terminal region (including segments flanking βI and the helix α) were reported in the NMR structures of monomeric βlg at acid pH [3], in agreement with the RMSF data in Fig. 6A. Thus, our study suggests that regions involved in the formation of the dimer interface are flexible in the free monomer at both acid and neutral pH.

Upon ligand binding, βlg underwent an overall structural rigidification (Fig. 6B). In particular, the β-strands, i.e., the walls of the binding cavity, consistently reduced their flexibility (Fig. 6A). This behavior contrasts with that reported for the self-association process of βlg [12,18]. Previous MD simulations suggested that dimerization induces an overall increase in the mobility of the protomers, a picture that is in qualitative agreement with infrared and Raman spectroscopic measurements [39]. Therefore, it can be anticipated that βlg has different ligand binding properties as a function of its aggregation state [40,41]. Disparate ligand-induced changes for the loops were observed in MD simulations. Loops AB and the C-terminal region reduced their mobility significantly, suggesting that ligand binding and self-association elicit similar effects on these zones of the protein. The flexibility of loop GH was also reduced upon ligand binding, whereas the loop EF seemed to be unaffected. This is at variance with results reported by Konuma et al. [15] who, on the basis of titration protocols monitored by heteronuclear NMR spectroscopy, concluded that residues at loops EF and GH, as well as at βD, increase their mobility in the presence of the ligand. However, the conformation exchange of these secondary structure elements was observed to increase on a time scale of μs to ms, i.e., much longer than that spanned in our MD runs.

Although it is difficult to rationalize the complicated behaviors observed in Fig. 6A, a structural analysis of the MD simulation trajectories provides some clues about the origins of differences among the three βlg structures. As indicated above, both the polar moieties and the aliphatic chains of DS and LA ligands occupied different average conformations in the βlg binding pocket along the simulations. This situation makes the ligands interact distinctly with different regions of the protein (Fig. 2). For instance, Lys[60] located at the end of βC and Lys[69] at the beginning of βD, interacted more readily with LA carboxylate than with DS sulfate. Furthermore, Leu[58], which also forms part of βC, interacted more with the aliphatic chain of LA than with that of DS (Figs. 2H and 4). These preferential interactions may explain why the movement of loop CD became more restricted in βlgLA compared to βlgDS. The aliphatic chains of both LA and DS

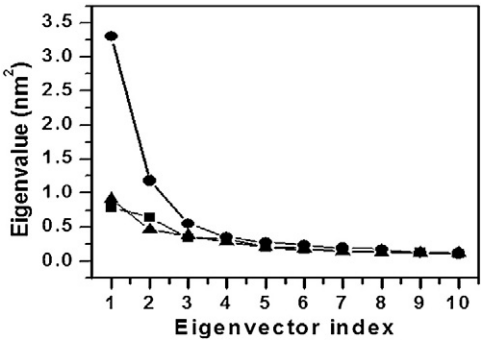

Fig. 7. Highest eigenvalues obtained from principal component analysis of the simulations for βlg_{apo} (circles), βlgLA (triangles) and βlgDS (squares).

established close hydrophobic contacts with Val[43] (Fig. 4), a residue located at the beginning of βB. This interaction could be responsible for the reduced conformational mobility of loop AB in both complexes (Fig. 6A). Nevertheless, DS also established hydrophobic contacts with Pro[38], Leu[39] and Val[41], interactions that were barely observed in βlgLA (Fig. 4). Therefore, these latter interactions could be responsible for the lower conformational mobility of loop AB in βlgDS.

A principal component analysis (PCA) of βlg and its ligand-bound forms was performed [31,42]. Although the motions dispersed over 1500 eigenvectors, 10 eigenvectors almost completely described the fluctuations in the three structures (Fig. 7). A similar result was obtained by Eberini et al. in their 3 ns-long MD study of βlg_{apo} and βlgPA [43]. As judged from the magnitudes of the first three eigenvectors, βlg_{apo} experienced the largest conformational fluctuations, in agreement with the RMSF results presented above.

In general, the distributions and amounts of coordinated motions along the first eigenvector were dissimilar among the three βlg structures. The amount of motion along the first eigenvector accounted for 57% of the overall fluctuations in βlg_{apo}, while it accounted for only 36% in the two ligand-bound forms. βlg_{apo} concentrated its motions on the loops AB, EF and GH, and the C-terminal region; βlgLA in the loops BC, DE and GH; and βlgDS in the loops GH, EF and AB (Fig. 8). The mobilities of loop AB and the C-terminus region were significantly restricted in the two complexes, in agreement with the RMSF results. In the three structures, loop GH showed a large mobility, although it was reduced in the presence of any of the two ligands. The displacement direction of loop GH depended on the ligand. While with LA it preserved the same direction than in βlg_{apo}, a different direction was observed with DS. According to the PCA, the mobility of loop EF in βlgDS showed a preferential displacement toward the interior of the binding cavity, a situation that contrasts with that in βlg_{apo}, where the same loop tended to displace towards the exterior of the molecule. This difference might be a result of the preferential interaction of DS with Asn[88] and Asn[90], in loop EF.

Overall, the PCA results also indicated that ligand binding induces an overall rigidification of the protein structure, although the extent and distribution of these effects depend on the particular ligand.

4. Conclusions

The formation energetics of βlgDS and βlgLA had previously been shown to vary drastically from each other [18]. LA binds to βlg driven by a large favorable entropic contribution, which is partially counterbalanced by an unfavorable enthalpy. In contrast, DS binding is both enthalpically and entropically driven. In the present study, MD techniques were used to gain insights into the structure and dynamics properties of apo and ligand-bound forms of monomeric βlg at neutral pH. Monomeric and dimeric subunits coexist nearly equimolar in cow's milk, indicating that both states are physiologically relevant [18,21]. However, βlg crystalizes only as a dimer at neutral pH, while heteronuclear NMR determinations have succeeded only when using a covalently linked form of the dimer. Thus, at the moment MD simulations are the only approach to study at atomic detail the structural features of monomeric βlg at neutral pH. Besides, the structure of βlgDS has not yet been solved experimentally.

The analysis presented herein revealed that βlg not only interacts distinctly with the polar moieties of LA and DS, but also with their aliphatic tails. Compared to LA's carboxylate, DS's sulfate is prone to form more lasting and cooperative hydrogen bonds with the protein. Furthermore, DS's aliphatic tail tends to penetrate deeper into the binding cavity than that of LA, allowing it to establish a larger number of hydrophobic contacts with the protein. Even in the absence of ligand, solvent does not penetrate into the hydrophobic region of the binding cavity. Thus, there is no energetic cost for dehydrating this part of the protein. As a consequence, the extra hydrophobic βlg-DS contacts that form at the bottom of the calyx may yield a favorable enthalpic contribution. Furthermore, the distinct interaction modes elicit different effects on the structural flexibility of the protein. The lesser penetration of the aliphatic tail, as well as the establishment of fewer contacts by the polar moiety, would be consistent with the higher entropy binding of LA. Therefore, it can be suggested that the binding energetic differences between the two ligands, i.e., the switch from a classical to a nonclassical hydrophobic effect, arises from distinctly optimized polar and hydrophobic contributions.

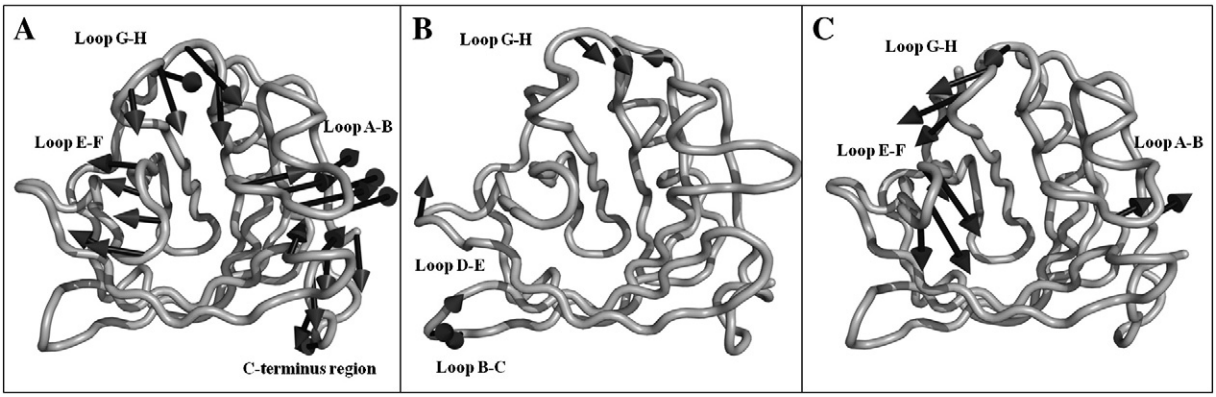

Fig. 8. Graphical representations of the two extreme projections along the first eigenvector of (A) βlg_{apo}, (B) βlgLA and (C) βlgDS. The direction and magnitude of motions are indicated by the arrows. Images were rendered by PyMOL 0.99rc6 [32].

Acknowledgment

This work was supported in part by DGAPA, UNAM [PAPIIT, IN204609, IN205712] and CONACyT [Grants 129239, 166472]. M.B. and G.G. received fellowships from CONACyT and DGAPA. Computer support and CPU time for the simulations were facilitated by DGTIC, UNAM.

References

[1] D.R. Flower, The lipocalin protein family: structure and function, Biochemical Journal 318 (1996) 1–14.
[2] B.Y. Qin, M.C. Bewley, L.K. Creamer, H.M. Baker, E.N. Baker, G.B. Jameson, Structural basis of the Tanford transition of bovine β-lactoglobulin, Biochemistry 37 (1998) 14014–14023.
[3] S. Uhrínová, M.H. Smith, G.B. Jameson, D. Uhrín, L. Sawyer, P.N. Barlow, Structural changes accompanying pH-induced dissociation of the β-lactoglobulin dimer, Biochemistry 39 (2000) 3565–3574.
[4] K. Sakurai, Y. Goto, Principal component analysis of the pH-dependent conformational transitions of bovine β-lactoglobulin monitored by heteronuclear NMR, Proceedings of the National Academy of Sciences of the United States of America 104 (2007) 15346–15351.
[5] J.J. Adams, B.F. Anderson, G.E. Norris, L.K. Creamer, G.B. Jameson, Structure of bovine β-lactoglobulin (variant A) at very low ionic strength, Journal of Structural Biology 154 (2006) 246–254.
[6] B.Y. Qin, L.K. Creamer, H.M. Baker, G.B. Jameson, 12 Bromododecanoic acid binds inside the calyx of bovine β-lactoglobulin, FEBS Letters 438 (1998) 272–278.
[7] S.Y. Wu, M.D. Perez, P. Puyol, L. Sawyer, β-lactoglobulin binds palmitate within its central cavity, Journal of Biological Chemistry 274 (1999) 170–174.
[8] G. Kontopidis, C. Holt, L. Sawyer, The ligand-binding site of bovine β-lactoglobulin: evidence for a function? Journal of Molecular Biology 318 (2002) 1043–1055.
[9] M.C. Yang, H.H. Guan, M.Y. Liu, Y.H. Lin, J.M. Yang, W.L. Chen, C.J. Chen, S.J. Mao, Crystal structure of a secondary vitamin D3 binding site of milk β-lactoglobulin, Proteins: Structure, Function, and Bioinformatics 71 (2008) 1197–1210.
[10] J. Loch, A. Polit, A. Gorecki, P. Bonarek, K. Kurpiewska, M. Dziedzicka-Wasylewska, K. Lewinski, Two modes of fatty acid binding to bovine beta-lactoglobulin-crystallographic and spectroscopic studies, Journal of Molecular Recognition 24 (2011) 341–349.
[11] H.A. McKenzie, W.H. Sawyer, Effect of pH on β-lactoglobulins, Nature 214 (1967) 1101–1104.
[12] M. Bello, G. Pérez-Hernández, D.A. Fernández-Velasco, R. Arreguín-Espinosa, E. García-Hernández, Energetics of protein homodimerization: effects of water sequestering on the formation of β-lactoglobulin dimer, Proteins: Structure, Function, and Bioinformatics 70 (2008) 1475–1487.
[13] F. Fogolari, L. Ragona, L. Zetta, S. Romagnoli, K.G. De Kruif, H. Molinari, Monomeric bovine β-lactoglobulin adopts a β-barrel fold at pH 2, FEBS Letters 436 (1998) 149–154.
[14] K. Sakurai, Y. Goto, Dynamics and mechanism of the Tanford transition of bovine β-lactoglobulin studied using heteronuclear NMR spectroscopy, Journal of Molecular Biology 356 (2006) 483–496.
[15] T. Konuma, K. Sakurai, Y. Goto, Promiscuous binding of ligands by β-lactoglobulin involves hydrophobic interactions and plasticity, Journal of Molecular Biology 368 (2007) 209–218.
[16] K. Sakurai, T. Konuma, M. Yagi, Y. Goto, Structural dynamics and folding of β-lactoglobulin probed by heteronuclear NMR, Biochimica et Biophysica Acta 1790 (2009) 527–537.
[17] L. Sawyer, β-lactoglobulin, in: P.F. Fox, P.L.H. McSweeney (Eds.), Advanced Dairy Chemistry, 3rd ed., Kluwer Academic/Plenum Publishers, 2003, pp. 319–386.
[18] M. Bello, M.D. Portillo-Téllez, E. García-Hernández, Energetics of ligand recognition and self-association of bovine β-lactoglobulin: differences between variants A and B, Biochemistry 50 (2011) 151–161.
[19] K.M.G. Oliveira, V.L. Valente-Mesquita, M.M. Botelho, L. Sawyer, S.T. Ferreira, I. Polikarpov, Crystal structures of bovine β-lactoglobulin in the orthorhombic space group C2221. Structural differences between genetic variants A and B and features of the Tanford transition, European Journal of Biochemistry 268 (2001) 477–483.
[20] N.R. Syme, C. Dennis, S.E.V. Phillips, S.W. Homans, Origin of heat capacity changes in a "nonclassical" hydrophobic interaction, ChemBioChem 8 (2007) 1509–1511.
[21] C.G. Prosser, S.A. Turner, R.D. McLaren, B. Langley, P.J. L'Huillier, P. Molan, M.J. Auldist, Milk whey protein concentration and mRNA associated with β-lactoglobulin phenotype, The Journal of Dairy Research 67 (2000) 287–293.
[22] T.L. McMeekin, B.D. Polis, E.S. DellaMonica, J.H. Custer, Crystalline compound of β-lactoglobulin with dodecyl sulfate, Journal of the American Chemical Society 71 (1949) 3606–3609.
[23] L.K. Creamer, Effect of sodium dodecyl sulfate and palmitic acid on the equilibrium unfolding of bovine β-lactoglobulin, Biochemistry 34 (1995) 7170–7176.
[24] C. Oostenbrink, A. Villa, A.E. Mark, W.F. van Gunsteren, A biomolecular force field based on the free enthalpy of hydration and solvation: the GROMOS force-field parameter sets 53A5 and 53A6, Journal of Computational Chemistry 25 (2004) 1656–1676.
[25] A.W. Schüttelkopf, D.M. van Aalten, PRODRG: a tool for high-throughput crystallography of protein–ligand complexes, Acta Crystallographica 60 (2004) 1355–1363.
[26] H.J.C. Berendsen, J.P.M. Postma, W.F. van Gunsteren, J. Hermans, Interaction models for water in relation to protein hydration, in: B. Pullman (Ed.), Intermolecular Forces, Reidel, Dordrecht, 1981, pp. 331–342.
[27] B. Hess, H. Bekker, H.J.C. Berendsen, J.G.E.M. Fraaije, LINCS: a linear constraint solver for molecular simulations, Journal of Computational Chemistry 18 (1997) 1463–1472.
[28] S. Miyamoto, P.A. Kollman, SETTLE: an analytical version of the SHAKE and RATTLE algorithm for rigid water models, Journal of Computational Chemistry 13 (1992) 952–962.
[29] H.J.C. Berendsen, J.P.M. Postma, W.F. van Gunsteren, A. Di Nola, J.R. Haak, Molecular dynamics with coupling to an external bath, Journal of Chemical Physics 81 (1984) 3684–3690.
[30] T. Darden, D. York, L. Pedersen, Particle mesh Ewald: An N*log (N) method for Ewald sums in large systems, Journal of Chemical Physics 98 (1993) 10089–10092.
[31] N. Díaz-Vergara, A. Piñeiro, Molecular dynamics study of triosephosphate isomerase from *Trypanosoma cruzi* in water/decane mixtures, The Journal of Physical Chemistry. B 112 (2008) 3529–3539.
[32] W.L. DeLano, The PyMOL Molecular Graphics System, DeLano Scientific, San Carlos, CA, USA, 2002 http://www.pymol.org.
[33] D. Frapin, E. Dufour, T. Haertle, Probing the fatty acid binding site of β-lactoglobulins, Journal of Protein Chemistry 12 (1993) 443–449.
[34] M.D. Pérez, P. Puyol, J.M. Ena, M. Calvo, Comparison of the ability to bind lipids of β-lactoglobulin and serum albumin of milk from ruminant and non-ruminant species, The Journal of Dairy Research 60 (1993) 55–63.
[35] G.B. Jeffrey, H. Maluszynska, A survey of hydrogen bond geometries in the crystal structures of amino acids, International Journal of Biological Macromolecules 4 (1982) 173–185.
[36] S. Brownlow, J.H.M. Cabral, R. Cooper, D.R. Flower, S.J. Yewdall, I. Polikarpov, A.C.T. North, L. Sawyer, Bovine β-lactoglobulin at 1.8 Å resolution-still an enigmatic lipocalin, Structure 5 (1997) 481–495.
[37] J. Qvist, M. Davidovic, D. Hamelberg, B. Halle, A dry ligand-binding cavity in a solvated protein, Proceedings of the National Academy of Sciences of the United States of America 105 (2008) 6296–6301.
[38] S.D. Sharrow, K.A. Edmonds, M.A. Goodman, M.V. Novotny, M.J. Stone, Thermodynamic consequences of disrupting a water-mediated hydrogen bond network in a protein:pheromone complex, Protein Science 14 (2005) 249–256.
[39] Y.M. Jung, B. Czarnik-Matusewicz, Y. Ozaki, Two-dimensional infrared, two-dimensional Raman, and two-dimensional infrared and Raman heterospectral correlation studies of secondary structure of β-lactoglobulin in buffer solutions, The Journal of Physical Chemistry. B 104 (2000) 7812–7817.
[40] Q. Wang, J.C. Allen, H.E. Swaisgood, Protein concentration dependence of palmitate binding to β-lactoglobulin, Journal of Dairy Science 81 (1998) 76–81.
[41] C. Jobichen, A.Z. Fernandis, A. Velázquez-Campoy, K.Y. Leung, Y.K. Mok, M.R. Wenk, J. Sivaraman, Identification and characterization of the lipid-binding property of GrlR, a locus of enterocyte effacement regulator, Biochemical Journal 420 (2009) 191–199.
[42] A. Amadei, A.B. Linssen, H.J.C. Berendsen, Essential dynamics of proteins, Proteins: Structure, Function, and Bioinformatics 17 (1993) 412–425.
[43] I. Eberini, M.A. Baptista, E. Gianazza, F. Fraternali, T. Beringhelli, Reorganization in apo and holo β-lactoglobulin upon protonation of Glu89: molecular dynamics and pKa calculations, Proteins: Structure, Function, and Bioinformatics 54 (2004) 744–758.
[44] A.C. Wallace, R.A. Laskowski, J.M. Thornton, LIGPLOT: a program to generate schematic diagrams of protein–ligand interactions, Protein Engineering 8 (1995) 127–134.